Different reaction behaviours of the light and heavy components of bio-oil during the hydrotreatment in a continuous pack-bed reactor

Mortaza Gholizadeh[a], Richard Gunawan[a], Xun Hu[a], Md Mahmudul Hasan[a], Sascha Kersten[b], Roel Westerhof[a], Weerawut Chaitwat[1,a], Chun-Zhu Li[*,a]

[a] Fuels and Energy Technology Institute, Curtin University of Technology, GPO Box U1987, Perth, WA 6845, Australia

[b] Sustainable Process Technology Group, Faculty of Science and Technology, University of Twente, Postbus217, 7500AE, Enschede, The Netherlands

Revised and submitted to

Fuel Processing Technology

For consideration for publication

[*]Corresponding author. Tel: (+) 61 8 9266 1131; Fax: (+) 61 8 9266 1138; E-mail: chun-zhu.li@curtin.edu.au

1 Present address: Environmental Engineering and Disaster Management Program, Mahidol University, Kanchanaburi Campus, Saiyok, Kanchanaburi, Thailand

Research highlights

- Hydrotreatment of bio-oil in a continuous packed-bed reactor was investigated.
- LHSV can drastically affect the hydrotreatment process.
- Lighter and heavier components in the same bio-oil could behave very differently.
- NiMo was less active for heavier species than lighter species.

Abstract

This study aims to investigate the hydrotreatment of bio-oil in a continuous packed-bed reactor at around 375°C and 70 bar. The bio-oil was produced from the grinding pyrolysis of mallee wood in a grinding pyrolysis pilot plant. Our results indicate that the lighter and heavier components in the same bio-oil could behave very differently. Their behaviour can be affected very significantly by the overall bio-oil liquid hourly space velocity. While the residence time of the light species that evaporate instantly could be very short, the residence time of heavy species passing through the catalyst bed in the form of liquid could be very long. When a commercial pre-sulphided NiMo/Al_2O_3 catalyst came into contact with the heavy bio-oil species, significant exothermic reactions would take place, which result in the deactivation of hyperactive sites in the catalyst. The NiMo/Al_2O_3 catalyst used was less active in hydrotreating the heavier bio-oil species than in hydrotreating the lighter bio-oil species. However, even at very low extents of hydrotreatment, the bio-oil structure and properties, e.g. coking propensity, could be drastically improved.

Keywords: Hydrotreatment; bio-oil; Light and Heavy Species; biofuel; LHSV.

1. Introduction

Increasing concerns about climate change and increasing demand for energy as a result of wide economic development, including that in rural and remote regions, have stimulated the development of various renewable energy technologies. Biomass holds a special position because biomass is the only carbon-containing renewable resource that can be used to produce liquid fuels to replace the petroleum-derived conventional ones. Pyrolysis of biomass would produce gases, biochar and bio-oil with their yields strongly depending on the feedstock and pyrolysis conditions [1-3]. Compared with the bulky biomass, bio-oil is a liquid that can be transported relatively easily and economically. This allows for the pyrolysis to be carried out in a modular and “distributed” mode, saving the costs to transport the wet bulky biomass over a long distance and greatly improving the economic competitiveness of biofuel production.

However, bio-oil is acidic and contains water and high molecular mass components [3-5]. Therefore, bio-oil cannot be used directly as a replacement of petrol and diesel. Bio-oil must be upgraded, e.g. via hydrotreatment [6-15]. During the hydrotreatment of bio-oil, a significant fraction of its oxygen will be removed in the forms of H_2O, CO and CO_2. The hydrotreatment could also result in decreases in molecular mass [13-14].

In order to improve the commercial feasibility of the hydrotreatment of bio-oil, the liquid hourly space velocity (LHSV) must be high enough so that the hydrotreatment reactor size can be reduced. The pressure of hydrogen should be as low as possible. LHSV, i.e. the rate at which bio-oil is fed into the hydrotreatment reactor, can significantly affect the formation of coke on the hydrotreatment catalyst, which

would ultimately result in the deactivation of the catalyst. Unfortunately, little information is available in the literature about the effects of LHSV on the product quality and coke formation, lagging behind the requirement of technology development.

As a product from the random thermal breakdown of macromolecular networks and other species in biomass, bio-oil has an inherently complicated composition with abundant reactive functional groups. More importantly, the bio-oil components would have a very wide molecular mass distribution with light species such as formic acid and heavy species that are the products from the partial thermal breakdown of the polymeric structures in biomass. During hydrotreatment, the residence time for bio-oil species could vary over an extremely wide range [15]. While some heavy bio-oil species would exist in the liquid phase in the hydrotreatment reactor, some would become vapour on entering the reactor. The overall LHSV value does not describe in any way the true residence time of various species in the reactor. This situation is worsened when operation is carried out at low pressures that is preferred to reduce the costs of biofuel production.

This study aims to investigate the behaviour of bio-oil during the hydrotreatment in a continuous reactor using a commercial pre-sulphided $NiMo/Al_2O_3$ catalyst at a moderate temperature (375°C) and a relatively low hydrogen pressure (70 bar). The study is focused on the effects of the overall LHSV on the hydrotreatment behaviour of lighter and heavier species in bio-oil. The hydrotreated products (termed as biofuel) were characterised with a wide range of analytical techniques in order to gain insights into the important processes taking place during hydrotreatment.

2. Experimental

2.1. Bio-oil sample

Bio-oil was produced in a grinding pyrolysis pilot plant [16,17] from the pyrolysis of mallee wood (Eucalyptus loxophleba, ssplissophloia) grown in the wheat belt of Western Australia [18,19]. Briefly, a mixture of wood chips having a wide range of particle sizes from microns to centimetres was continuously fed into a rotating reactor at 450°C in which the pyrolysis and particle size reduction took place simultaneously. After the separation of biochar particles in two cyclones, bio-oil vapour was condensed to give the liquid bio-oil sample used in this study. The bio-oil sample was stored in a freezer (-18°C) until use. The bio-oil was filtered (20-25µm) before the hydrotreatment experiments.

2.2. Hydrotreatment

The hydrotreatment of bio-oil was carried out in a U-shape continuous pack-bed reactor, as is shown in Figure 1. The reactor was made of stainless steel 316 and had a diameter of 3/4 inch with a total reactor length of 40 cm. The reactor was partly (about half, see “the sand bath level” shown in Figure 1) immersed in a hot fluidised sand bath that was heated to 375°C. The U-shaped reactor design made it easier to heat up the reactor in a sand bath. The packed-bed reactor contains two zones of catalysts. In the first zone (10 cm), 5% palladium supported on activated carbon (Pd/C, Bioscientific) catalyst was used. It was outside the sand bath. This section would have undergone a temperature transition ranging from room temperature to <250°C, aiming to stabilise the incoming bio-oil based on the finding in the literature

[20]. However, as will be demonstrated later in this paper, the use of Pd/C catalyst was marginally, if any, successful in avoiding coke formation. In the second zone, a commercial pre-sulphided $NiMo/Al_2O_3$ catalyst (from Eurecat, hereafter referred as "NiMo catalyst") was used. This section of the catalyst was immersed in the hot fluidised sand bath. The steady-state temperature at the border of the Pd/C and NiMo catalyst beds was between 235 and 270°C under current experimental conditions.

The process flow diagram of this hydrotreatment set up has been shown elsewhere [15]. The bio-oil and hydrogen was pre-mixed before being fed into the reactor. The bio-oil was pumped, at a pre-set constant flow rate, into the reactor using a syringe pump (Teledyne Isco, 500D). The LHSV was defined as the ratio between the bio-oil feeding rate and the volume of the catalyst bed (i.e. the volume of the reactor occupied by the catalyst). The LHSV was increased by increasing the bio-oil feeding rate. The LHSV for the NiMo catalyst was varied between 1 and 3 hr^{-1} in separate experiments. The LHSV for the Pd/C catalyst would be twice that for the NiMo catalyst for the same experiment. Hydrogen was supplied in large excesses via a mass flow controller at a constant flow rate of 4 L/min (measured under ambient conditions) for all experiments.

Two thermocouples were inserted into the catalyst bed to measure the catalyst temperature during the experiments. The tip of the first one was placed 5 cm at the inlet side below the surface level of the fluidised sand bath. The tip of the second thermocouple was also 5 cm, but at the outlet side, below the surface level of the fluidised sand bath. The distance between the tips of the two thermocouples in the flow direction was 10 cm.

The pressure at the outlet of the reactor was maintained at 70 bar by using a back pressure regulator (EquilibarEB1HP2) installed after the condenser system of two parallel traps. The temperature of the condenser system at its outlet was maintained below 10°C by cooling the traps with ice water. The hydrotreated liquid products were collected into fractions every 45 min ($LHSV_{NiMo}$ = 2), 60 min (LHSV = 3) or 90 min (LHSV = 1). The samples were then stored at -18°C and were de-frozen prior to analysis.

The hydrotreated product was normally separated into two phases. The total water production is calculated as the sum of water in the aqueous and oil phases minus the water in the feed bio-oil. The yield of each product was expressed as the mass of product (e.g. the whole biofuel product or certain fraction) divided by the mass of bio-oil fed into the reactor over the same time interval. The product yields are always expressed on the basis of moisture-free (mf) bio-oil feedstock.

2.3. Product characterisation

UV-fluorescence spectroscopy. UV-fluorescence spectroscopy was used to understand the transformation of aromatic structures during hydrotreatment. A Perkin-Elmer LS50B spectrometer was used to measure the UV-fluorescence spectra of bio-oil and its hydrotreated products. Samples were diluted with UV grade methanol (purity ≥ 99.9%) to 4 ppm (wet basis). The energy difference for recording synchronous fluorescence spectra was -2800 cm^{-1} with slit widths of 2.5 nm (excitation and emission) and a scanning speed 200 nm/min. The fluorescence intensity was multiplied by the product oil yield to express the fluorescence intensity on the basis of bio-oil (moisture-free) to allow for comparison [21].

GC-MS. The raw bio-oil and the product oil phase were analysed with Agilent GC-MS (a 6890 series gas chromatograph with a 5973 mass spectrometric detector) equipped with a capillary column (HP-INNOWax) (length, 30 m; internal diameter, 0.25 mm; film thickness, 0.25 µm of crosslinked polyethylene glycol) [4,5,22]. The samples were diluted with acetone prior to analysis [10,15]. The following compounds were quantified: acetic acid, phenol, 2-ethyl-phenol, 2,4,6-trimethyl-phenol, 2,4-dimethyl-phenol, 4-(1-methylpropyl)-phenol and 3,4,5-trimethyl-phenol. The phenolic type of compounds are summed together and hereafter referred to as phenolics. Another group of compounds quantified included ethylbenzene, 1,3-dimethyl-benzene, 1,2-dimethyl-benzene, 1,4-dimethyl-benzene, propyl-benzene, 1-ethyl-2-methyl-benzene, 1,2,3-trimethyl-benzene and (1-methylpropyl)-benzene, which are summed together and referred to as benzene compounds. Cyclopentaneandmethyl-cyclohexane were also quantified.

Thermogravimetric analysis (TGA) was used to gauge the volatility of hydrotreated products, which partially reflects the molecular mass distribution. The weight loss and differential thermogravimetric (DTG) curves of hydrotreated bio-oils (biofuels) were measured using a TGA (TA Instruments Q5000). The samples were heated from 25 to 500°C at a heating rate of 10°C min^{-1} in a flow of nitrogen (50 mL min^{-1}) [3-5,23]. After the experiment, the residue, as a result of the evaporation of light species and polymerisation, was measured and is referred to as “potential coke”.

Elemental analysis. A Thermo Flash 2000 analyser was used for the elemental analysis (C,H and N) of the bio-oil and biofuel samples. The oxygen content was calculated by difference [24].

3. Results and discussion

3.1. General observation

Reproducibility. To check the reproducibility of our experiments, one set of two experiments under identical conditions (LHSV = 1 hr^{-1}) were performed. It was found that both the temperature and pressure profiles were almost identical. The product yields on the moisture-free basis from these two repeated experiments were as follows after feeding 256 mL of bio-oil into the reactor. Yields of the organics in the oil phase were 23.8 and 20.8wt%, respectively. Yields of the organics in the aqueous phase were 9.5 and 6.6wt%, respectively. Yields of the produced water were 31.9 and 37.2wt%, respectively. Yields of the accumulated gas and coke was 34.8 and 35.4wt%, respectively.

The pressure drop across the reactor would remain low (<4 bar) initially but then increased rather rapidly, despite of the use of Pd/C catalyst at the beginning of the catalyst bed (Figure 1). Once the pressure increased very significantly (e.g. >110 bars), the experiments were terminated. Contrary to the reports in the literature [20,25] that the Pd/C catalyst could stabilise the bio-oil to reduce coke formation, these experiments demonstrated that the stabilisation of bio-oil using the Pd/C catalyst was rather limited, certainly not to the extent to ensure long-term continuous operation using the NiMo catalyst, at least under the current experimental conditions. In fact, separate experiments [15,17] also showed that the use of Pd/C alone (i.e. without the NiMo catalyst) would also result in the blockage of reactor and the deactivation of catalyst.

Exothermic peaks. As is shown in Figure 1, two thermocouples were placed in the NiMo catalyst bed: one at 5 cm into the NiMo catalyst bed in the fluid flow direction and another one at 15 cm into the bed. The bed temperatures measured at 15 cm into the NiMo catalyst bed for the three different LHSV values are shown in Figure 2a. The x-axis refers to the total amount of bio-oil that had been fed into the reactor, which facilitates a better comparison of the experiments with different bio-oil feeding rates. It is an indirect indication of the time that has passed since the start of the feeding of bio-oil. Figure 2b shows the temperature profiles measured at 5 and 15 cm into the NiMo catalyst bed at the same LHSV value of 3 hr^{-1}.

The most striking feature of Figure 2 is the presence of huge exothermic peaks. Temperature increases as high as 80°C were observed. Under the present experimental conditions (>350°C and >70 bar), many light species (e.g. acetic acid with a critical temperature of 319.6°C) would exist in the gas/vapour phase. Carried by the excess supply of hydrogen, the residence time of these light species could be at the order of seconds, in fact <0.8 s in this particular case. However, the data in Figure 2 indicate that, at 5 cm in the catalyst bed, it took many minutes for the exothermic peaks to appear. Therefore, it is fair to conclude that the exothermic peaks were not due to the hydrotreatment of light species that would travel through the reactor in the gas/vapour phase. Instead, these exothermic peaks were due to the hydrotreatment of the bio-oil species that largely travelled through the catalyst bed in the reactor in the liquid phase.

The presence of a peak in Figure 2 would mean that the exothermic reactions at the given location where the thermocouple was present underwent increases and decreases in reaction rates (i.e. the heat generation rate) with time. However, bio-oil was always continuously fed into the reactor at a pre-set constant flow rate in each

experiment in the continuous excess supply of hydrogen. Any hydrotreatment reactions at a given location in the catalyst bed would be expected to show increases in reaction rates (as the reactants were supplied to, i.e. reached, the catalyst at that given location) and then level off (i.e. not to decrease). In other words, the reaction rates at a given location in the catalyst bed should have shown a monotonic increase and then approached a plateau value without showing a maximum. One plausible explanation to this apparent contradiction between the observed reaction rate peaks (exothermic peaks) and the expected monotonic-plateau trends is that (part of) the catalyst was almost instantly deactivated to result in decreases in the reaction rate (i.e. heat generation rate). An alternative explanation is that the changes in the heat transfer as the surrounding medium changed vapour/gas-dominating to a mixture of vapour/gas-liquid mixture might have also contributed to the observed peaks. However, the second possibility appeared much less likely because the peaks were very broad. Therefore the first explanation, i.e. catalyst deactivation, appeared more likely. As will be shown later, the bio-oil was continuously hydrotreated well beyond the time scale of the exothermic peaks shown in Figure 2. Therefore, the catalyst deactivation associated with the exothermic peaks in Figure 2 was very selective. In other words, only a (small) fraction of the hyperactive sites in the catalyst were instantly deactivated as soon as they came into contact with (some components of) the bio-oil.

A further observation can be made from the data in Figure 2a. As the bio-oil feeding rate was increased (i.e. as the LHSV was increased), the liquid components reached the location at 15 cm in the NiMo catalyst bed increasingly rapidly. While the exothermic peak appeared after 270 mL of bio-oil was fed into the reactor (470 min) at a LHSV of 1 hr^{-1}, the exothermic peaks showed at about 150 mL (130 min) and

110 mL (65 min) for LHSVs of 2 and 3 hr^{-1} respectively. In other words, the exothermic peak did not show after the same amount of bio-oil was fed into the reactor at different bio-oil feeding rates. The exothermic peak became increasingly narrow and high as the LHSV was increased from 1 to 3 hr^{-1}. Clearly, the hydrotreatment reactions would take place as soon as the bio-oil and hydrogen came into contact with the catalyst. In addition to, or simultaneously with, the removal of oxygen from bio-oil, the molecular sizes would also decrease, which combine to turn more bio-oil components into vapour. With decreasing LHSV value, the residence time of bio-oil in the reactor would increase for more hydrotreatment reactions to take place. The net result is that the actual liquid flow rate in the downstream decreased more than the decreases in the bio-oil feeding rate. Another reason for the exothermic peak not to appear after the same amount of bio-oil was fed at different feeding rates was due to the need for the liquid to fill the pores in the catalyst. Certain amount of liquid must be required to fill the pores within the catalyst particles. Once the liquid molecules went into pores, they were less carried ("blown") by the gas and liquid and thus moved through the reactor slowly. Once the pores are filled, the extra liquid would be forced by the flowing hydrogen through the reactor more rapidly.

It then follows that the composition of liquid/vapour reaching the catalyst downstream, e.g. at the location of 15 cm into the catalyst bed in Figure 2a, would be different when LHSV value was increased. Nevertheless, the exothermic peak always appeared. As will be shown later (Figure 5), the overall oxygen content of the liquid passing through the catalyst bed at 15 cm would be very different as the LHSV value was increased. While the hyperactive sites in the catalyst at that location (15 cm) would complete the deactivation only after the residual liquid from about 150-

200 mL (peak width in Figure 2a) of bio-oil had passed by at an LHSV of 1 hr^{-1}, the peak width was only about 70-80 mL in the case of LHSV of 3 hr^{-1}. All results combine to indicate that the deactivation of hyperactive sites in the catalyst, as was evidenced by the exothermic peaks, is related both to the catalyst itself (heterogeneity in terms of the presence of some hyperactive sites) and to the bio-oil composition.

3.2. Overall product yields

The effects of LHSV on the yield of organic products from the hydrotreatment of bio-oil are shown in Figure 3. The product stream from the hydrotreatment reactor went alternatively into one of two traps to condense the liquid products. The product was thus collected into time-on-stream-resolved fractions. Each datum point in Figure 3 (and other figures) represented the yield of product collected in one trap, which was defined as the amount of product in the trap divided by the amount of bio-oil (on the moisture-free basis) fed into the reactor over the same period of time. To determine the amount of product in a trap, the trap contents were then transferred into a container where the product separated into two phases: one oil phase rich in organic product and one aqueous phase rich in water. The amount of each phase was weighed following decanting. The water content in each phase was determined to calculate the amount of organics in each phase (shown as “in oil phase” and “in aqueous phase” in Figure 3). The total yield of organics in the whole trap is also shown in Figure 3. The product in the first trap contained impurities (e.g. the solvent residue used to clean the feeding line) and thus was not considered in plotting the data in Figure 3. The transfer of the contents in a pressurised trap into another

container at atmospheric pressure was a difficult operation and did not always ensure 100% transfer of all materials in the trap. This contributed significantly to the observed scatters in the data shown in Figure 3.

The total yields of organic products during the initial periods of hydrotreatment were low, often <30%. The low liquid product yields were neither due to the formation of coke nor due to the formation of gases. Massive formation of coke at this level would have blocked the reactor: the observed pressure drop increases were in fact minimal. Furthermore, the analysis of gases using a gas chromatograph did not give evidence of massive gas formation. When the total yield of water formation was considered (Figure 4), the total yield of organics and water was far smaller than 90%. The main reason must be due to the hold up of liquid in the catalyst bed in the reactor. In fact, little product (although difficult to quantify accurately, see above) was collected in the first trap. Significant amounts of heavier bio-oil components, as liquid, filled the pores in the catalyst particle and the inter-particle voids in the reactor. The hold up of bio-oil components in the reactor has been observed and discussed in detail in our previous study [15].

It follows then that the organic products observed in the first couple of traps are mainly the light species (also see discussion below) that travelled through the reactor in the gas/vapour phase. These species were well hydrotreated to form water (Figure 4) and to give products with low oxygen contents (Figure 5). Irrespective of the LHSV values used in the range of 1 to 3 hr^{-1}, the oxygen contents of the products in the oil phase at the initial stages of the experiments (low amount of bio-oil fed into the reactor) were very low (Figure 5). It can thus be concluded that the NiMo catalyst was very active to hydro-deoxygenate the species in the gas/vapour phase, at least under the current experimental conditions.

At a LHSV value of 1 hr^{-1}, the observed yield of organics, mainly that in the oil phase, increased rapidly to about 30 wt% of bio-oil fed into the reactor (on the moisture-free basis). This is at least partly due to the appearance of heavier species in the product stream when the catalyst bed had been saturated with the heavy liquid. The yield of organic product and the production of water remained almost unchanged (within the scatters) until after ~500 mL of bio-oil had been fed into the reactor. Beyond 500 mL of bio-oil feed, the yield of organic product increased (Figure 3), which was accompanied by the increases in its oxygen content (Figure 5) and somewhat by the decreases in the production of water (Figure 4). This signals the deactivation of catalyst for reduced hydro-deoxygenating activities.

When the LHSV value was increased to 2 and 3 hr^{-1}, the yield of organic products appeared to increase more rapidly and to a higher value (to 60-70wt%) than at 1 hr^{-1}, with less water production and higher oxygen content in the oil phase. At an LHSV value of 1 hr^{-1}, the reaction was stopped due to coke formation and reactor blockage before reaching plateau values.

These data would indicate that the NiMo catalyst used in the present study appeared to have less ability to handle heavy bio-oil components than the lighter ones. The behaviour of lighter and heavier species will be discussed below.

3.3. The transformation and formation of lighter compounds in the vapour phase

Figure 6 shows the yields of various classes of lighter species in the products. In each case, those found in the aqueous and oil phases were summed up to give the total yields shown in Figure 6. The datum points at “0 mL” of bio-oil fed into the

reactor indicates the contents of these species in the raw bio-oil. Due to the complexity of bio-oil composition, many species may be formed and consumed simultaneously during the hydrotreatment. For simplicity, all species have been shown as “yield”, which should simply be taken as a ratio of their mass flow rate at the reactor exit to the bio-oil feeding rate.

Acetic acid is the most abundant (up to 15wt%) organic acid in bio-oil, contributing to the high acidity of the unhydrotreated bio-oil. The data in Figure 6a show that acetic acid can be destroyed/converted during hydrotreatment, improving the biofuel product quality. The exact products from acetic acid remain unclear, which may include CO_2 and hydrogenated products such as methanol. Part of acetic acid structure (e.g. CH3) may also be incorporated into the hydrotreatment products. At all LHSV values used, acetic acid was nearly completely destroyed/converted during the initial periods of the experiments. It is believed that acetic acid would exist in the vapour form under the present experimental conditions and thus would travel through the reactor rapidly. This means that the fresh NiMo catalyst was very active in removing acetic acid. However, the concentration (reflected as “yield”) of acetic acid increased as the experiment progressed, increasing more rapidly at a higher LHSV value than at a lower LHSV value. At a LHSV value of 1 hr^{-1}, significant amounts of acetic acid were observed after >400 mL of bio-oil had been fed into the reactor. This appears to coincide with the exothermic peak shown in Figure 2a: by extrapolation, the exothermic peak would appear at the end of the NiMo bed at >400-500 mL. Even at the end of that experiment, the concentration of acetic acid in the product was never as high as its concentration in the raw bio-oil. This is taken to mean that the destruction of acetic acid can take place both at the hyperactive sites and at the “normal” active sites of the catalyst. However, the occupation of the

reactive sites by heavy liquid species did greatly reduce the accessibility of these active sites to acetic acid.

When the LHSV was increased to 2 hr^{-1}, acetic acid started to appear in the product stream just after 350 mL of bio-oil had been fed into the reactor. At the LHSV value of 3 hr^{-1}, acetic acid appeared in all product samples except in the product in the first trap. These again correspond to Figure 2a that the exothermic peaks appeared earlier with increasing LHSV. These results confirm the importance of availability of active sites to the destruction of acetic acid, which could be occupied by the heavy species.

Figure 6b shows the yield of phenolics including phenol and substitutional phenols. Figure 6c shows the yields of benzene and substituted benzenes, shown as “benzene compounds”. Bio-oil is rich in phenol structures both as light components and as heavy components, including lignin-derived oligomers [3,4,21]. However, many phenol structures in bio-oil were embedded in large molecules that would not have gone through the GC column to be quantified. Therefore, light phenolics could be converted, e.g. to produce benzene and substitutional benzenes, or formed from the breakdown of lignin-derived oligomers. Indeed, the content of GC-quantified light phenolics in bio-oil was higher than the yield of phenolics in the oil phase products produced at the earlier stages at LHSVs of 1 or 2 hr^{-1} but lower than the yields under all other conditions. The data in Figures 6b and 6c indicate that the fresh NiMo catalyst at the initial periods of experiments was active in converting light vapour phenolics (Figure 6b) into benzene compounds. At the later periods of experiments, this conversion was a lot less effective. This must again have been due to the occupation of the catalyst active sites by the heavy species. In some cases, e.g. LHSV of 2 hr^{-1}, when the catalyst was significantly deactivated at later stages of

experiments, the observed yields of GC-quantified phenolics decreased, apparently owing to the reduced conversion of phenol structures in large molecules into GC-quantified light phenolics. In the case of LHSV of 3 hr^{-1}, the low yields of GC-quantified phenolics must have been due to the low activities of the catalyst that were in contact with abundant bio-oil liquids even at the earlier periods of experiments. To produce high yields of benzene compounds, the catalyst must be sufficiently active to produce light phenolics and also convert light phenolics into benzene and substitutional benzenes, explaining the trends in Figure 6c. For example, at a LHSV value of 3 hr^{-1}, the active sites were not sufficiently available to convert the phenol structure in large molecules into light phenolics (Figure 6b) or to convert the light phenolics into benzene compounds, with the exception at the beginning of the experiment.

Substituted cyclopentanes and cyclohexanes are the hydrogenation products. As is shown in Figure 6d, their production was favoured at the fresh catalyst surface, mostly from the hydrogenation of light species in the gas/vapour phase, and decreased with the occupation of the catalyst by liquid and the deactivation of the catalyst.

3.4. Transformation of structure and properties of bio-oil during hydrotreatment

Observation based on TGA. Thermogravimetric analysis was used to characterise the thermal properties of the hydrotreated products. A small amount of the oil phase product was heated up in a TGA to 500°C at a heating rate of 10°C/min. The weight loss was a result of combined physical (evaporation) and chemical (decomposition)

processes, which in turn is partly related to the molecular mass distribution (see below). The residue at 500°C was termed as “potential coke”, reflecting the potential amount of coke that would form when the oil is heated to 500°C. Figure 7 shows the typical DTG curves and the potential coke yields of the hydrotreated oil products (in the oil phases) in comparison with those of the raw bio-oil. The TGA was carried out only with the oil phase products because of the difficulties in getting accurate data with the aqueous phases that had very high water contents.

The data in Figure 7a show that, at a LHSV value of 2 hr^{-1}, the product collected initially (after only 205 mL of bio-oil was fed) was relatively light, all evaporated at<225°C in TGA with almost no solid residue (potential coke) left at 500°C in TGA (Figure 7b). With the progress in hydrotreatment, the product became heavier, requiring higher temperature to evaporation TGA. Some solid residue started to appear (Figure 7b) for the product collected after 350 mL of bio-oil was fed into the hydrotreatment reactor; the potential yield increased rapidly thereafter. Nevertheless, the potential coke yields of the hydrotreated oil products were always less than that of the raw bio-oil. In fact, the data in Figure 7a show that the hydrotreated oil phase contained species heavier than those in the raw bio-oil, as is evidenced by the high DTG intensity at >400°C in TGA. However, caution must be exercised in interpreting the DTG data at high temperatures (e.g. >300°C). Bio-oil is exceedingly reactive and will polymerise once it is heated up to elevated temperatures [26]. At high temperatures, these species would tend to polymerise instead of being evaporated, giving very high potential coke yield. On the other hand, many O-containing functional groups responsible for the high reactivity of bio-oil would have been hydro-deoxygenated. Therefore, the data in Figure 7 indicate that the hydrotreated bio-oils, even at the later stages of experiments when the catalyst has been partially blocked

or even partially deactivated, have much less tendency to polymerise than the raw bio-oil. Some species in the hydrotreated bio-oil could still evaporate at >450°C instead of forming coke.

The data in Figure 7b indicate that the potential coke yield determined in TGA was always low for the LHSV value of 1 hr^{-1}. Increasing LHSV resulted in rapid increases in the potential coke yield. This is at least due to two reasons. Firstly, the residence time decreased with increasing LHSV, giving less time for hydrotreatment reactions to take place. Secondly, the concentration of heavy liquid in the reactor increased with increasing LHSV, limiting the access of active sites to hydrogen. In the absence of abundant active hydrogen, the relative importance of polymerisation would increase over the hydrogenation and hydrocracking reactions, favouring the formation of heavy species and coke.

Transformation of aromatic structures as reveal by UV-fluorescence spectroscopy. Figure 8 shows the synchronous spectra of hydrotreated bio-oils (oil phases). As was stated in Experimental, the fluorescence intensity has been expressed on the basis of moisture-free bio-oil to allow for comparison under different experimental conditions. The spectrum for the raw bio-oil is shown for comparison. At the initial stages of hydrotreatment (Sample 1, Figure 8a), the fluorescence intensity was generally very low. Little intensity was observed at wave lengths longer than 320 nm, signalling the absence of ring structures with more than 2 (equivalent) fused benzene rings. The lack of oxygen in the hydrotreated bio-oil also would not give high quantum yields, contributing to the observed low intensity. These data are taken to indicate that the gas-phase-dominated hydrotreatment product was well hydrotreated. This is in agreement with the visual observation that

these samples were lightly coloured.

With the progress of experiments (e.g. Sample 2 in Figure 8b), the fluorescence intensity increased, at least partly due to the appearance of liquid that had travelled through (most of) the catalyst bed. In particular, at the LHSV value of 3 hr^{-1}, there was a significant increase in fluorescence intensity at wavelengths longer than 300 nm, most likely due to the aromatic structures with more than 2 (equivalent) fused benzene rings.

At the later stages of experiments (Samples 3 and 4 in Figures 8c and 8d), the observed fluorescence intensity of the hydrotreated bio-oils were similar to or higher than those of the raw bio-oil. However, the similarities in the spectral features between the raw and hydrotreated bio-oils (e.g. the shoulder peaks at around 385 nm) indicate the similarities in their aromatic structure features. The explanation of these data must consider the importance of intra-molecular energy-transfer to the observed fluorescence intensity for this type of samples [27]. Due to the intra-molecular energy transfer, very large aromatic ring systems in large molecules in bio-oil are not well represented by the observed fluorescence [27]. As these large molecules are broken down as a result of thermal or hydrocracking or removal of oxygen, the efficiency of intra-molecular transfer is lowered to result in a better representation of these large aromatic ring systems in the observed fluorescence. This explains why the fluorescence intensity of hydrotreated bio-oil can be higher than that of the raw bio-oil, but having similar spectral features. The possible formation of additional aromatic structures during the later stage of hydrotreatment cannot be ruled out but our data do not give conclusive evidence for this possibility.

The UV-fluorescence data in Figure 8 further support the discussion above in that the lighter species have behaved differently from the heavier species. The

catalyst became increasing less effective in hydrogenating the aromatic structures.

4. Conclusions

The continuous hydrotreatment of bio-oil in a packed bed catalytic reactor using a presulphided NiMo/γ-Al_2O_3 catalyst was carried out under mild conditions (375°C, 70-80 bar). The aim was to investigate the hydrotreatment behaviour of the light and heavy components as a function of LHSV and catalyst time-on-stream. Our results indicate that the lighter and heavier components in the same bio-oil could behave very differently. The overall bio-oil liquid hourly space velocity can drastically affect the hydrotreatment process. While the residence time of the light species that evaporate instantly could be very short, the residence time of heavy species could be very long as they passed through the catalyst bed in the form of liquid. The initial contact of heavy bio-oil species with the pre-sulphided NiMo/Al_2O_3 catalyst could result in very significant exothermic peaks but did not create a thermal runaway situation, owing to the rapid deactivation of the hyperactive sites in the catalyst. The NiMo catalyst used was less active in hydrotreating the heavier bio-oil species than in hydrotreating the lighter bio-oil species. The potential coke yields of the hydrotreated bio-oils, even at very low extents of hydrotreatment, were drastically reduced.

Acknowledgements

This project received funding from ARENA as part of ARENA's Emerging Renewables Program and the Second Generation Biofuels Research and Development Grant Program. The study also received support from the Government

of Western Australia via the Low Emissions Energy Development Fund and via the Centre for Research into Energy for Sustainable Transport (CREST).This research used large samples of mallee biomass supplied without cost by David Pass and Wendy Hobley from their property in the West Brookton district.

References

[1] A.V. Bridgwater, D. Meier, D. Radlein, An overview of fast pyrolysis of biomass. Organic Geochemistry 30 (1999) 1479-1493.

[2] D. Mohan, C.U. Pittman, P.H. Steele, Pyrolysis of wood/biomass for bio-oil: A critical review. Energy & Fuels 20 (2006) 848-889.

[3] M. Garcia-Perez, X.S. Wang, J. Shen, M.J. Rhodes, F.J. Tian, W.J. Lee, H. Wu, C.-Z. Li, Fast pyrolysis of oil mallee woody biomass: Effect of temperature on the yield and quality of pyrolysis products. Industrial & Engineering Chemistry Research 47 (2008) 1846-1854.

[4] M. Garcia-Perez, A. Chaala, H. Pakdel, D. Kretschmer, C. Roy, Characterization of bio-oils in chemical families. Biomass & Bioenergy 31 (2007) 222-242.

[5] M. Garcia-Perez, S. Wang, J. Shen, M. Rhodes, W.J. Lee, C.-Z. Li, Effects of temperature on the formation of lignin-derived oligomers during the fast pyrolysis of mallee woody biomass. Energy & Fuels 22 (2008) 2022-2032.

[6] D.C. Elliott, Historical developments in hydroprocessing bio-oils. Energy & Fuels 21 (2007) 1792-1815.

[7] W. Baldauf, U. Balfanz, M. Rupp, Upgrading of flash pyrolysis oil and utilization in refineries. Biomass & Bioenergy 7 (1994) 237-244.

[8] A. Zacher, M. Olarte, D. Santosa, D.C. Elliot, B. Jones, A review and perspective of recent bio-oil hydrotreating research. Green Chemistry 16 (2014) 491-515.

[9] R.H. Venderbosch, A.R. Ardiyanti, J. Wildschut, A. Oasmaa, H.J. Heeres, Stabilization of biomass-derived pyrolysis oils. Journal of Chemical technology and & Biotechnology 85 (2010) 674-686.

[10] R. Gunawan R, L. Xiang, C. Lievens, M. Gholizadeh, W. Chaiwat, X. Hu, D. Mourant, J. Brombly, C.-Z. Li, Upgrading of bio-oil into advanced biofuels and

chemicals. Part I. Transformation of GC-detectable light species during the hydro treatment of bio-oil using Pd/C catalyst. Fuel 111 (2013) 709-717.

[11] E.G. Baker, D.C. Elliott, Catalytic hydrotreating of biomass-derived oil, in: E.J. Soltes, T.A. Milne (Eds.), Pyrolysis oils from biomass, ACS symposium series, Washington, 1988, p. 228-240.

[12] E.G. Baker, D.C. Elliott, Catalytic upgrading of biomass pyrolysis oils, in: A.V. Bridgewater, J.L. Kuester (Eds.), Research in thermochemical biomass conversion, Springer Netherlands, Washington, 1988, p.883-895.

[13] D.C. Elliot, T.R. Hart, G.G. Neuenschwander, L.G. Rotness,A.H. Zacher, Catalytic hydroprocessing of biomass fast pyrolysis bio-oil to produce hydrocarbon products. Progress and Sustainable Energy 28 (2009) 441-449.

[14] M.F. Miguel, F. Mercader, P.J.J. Koehorst, H.J. Heeres, S.R.A. Kersten, J.A. Hogendoorn, Competition between hydrotreating and polymerization reactions during pyrolysis oil hydrodeoxygenation. AIChE Journal 57 (2011) 3160-3170.

[15] W. Chaiwat, R. Gunawan, M. Gholizadeh, X. Li, C. Lievens, X. Hu, Y. Wang, D. Mourant, A. Rossiter, J. Brombly, C.-Z. Li, Upgrading of bio-oil into advanced biofuels and chemicals. Part II. Importance of holdup of heavy species during the hydrotreatment of bio-oil in a continuous packed-bed catalyst reactor. Fuel 112 (2013) 302-310.

[16] C.-Z. Li, X. Wang, H. Wu, Method of and system for grinding pyrolysis of particulate carbonaceous feedstock, PCT/AU 2011/000741 (provisional application no: 2010902743; on 22 June 2010); Owner: Curtin University of Technology.

[17] M. M. Hasan, Pyrolysis behaviour of mallee biomass, March 2015: Curtin University of Technology.

[18] D. Cooper, G. Olsen, J. Bartle, Capture of agricultural surplus water determines

the productivity and scale of new low-rainfall woody crop industries, Australian Journal of Experimental Agriculture 45 (2005) 1369-1388.

[19] J. Bartle, G. Olsen, D. Cooper, T. Hobbs, Scale of biomass production from new woody crops for salinity control in dryland agriculture in Australia, International Journal of Global Energy Issues 27 (2007) 115-137.

[20] D.C. Elliott, E.G. Baker, Process for upgrading of biomass pyrolyzates, patentno: 4; in: USA (1989) pp.7.

[21] Y. Wang Y, X. Li, D. Mourant, R. Gunawan, S. Zhang, C.-Z. Li, Formation of aromaticstructures during the pyrolysis of bio-oil. Energy & Fuels 26 (2011) 241-247.

[22] M.C. Samolada, W. Baldauf, I.A. Vasalos, Production of a bio-gasoline by upgrading biomass flash pyrolysis liquids via hydrogen processing and catalytic cracking. Fuel 77 (1998) 1667-1675.

[23] X. Li, R. Gunawan, C. Lievens, Y. Wang, D. Mourant, S. Wang, H. Wu, M. Garcia Perez, C.-Z. Li, Simultaneous catalytic esterification of carboxylic acids and acetalisation of aldehydes in a fast pyrolysis bio-oil from mallee biomass. Fuel 90 (2011) 2530-2537.

[24] R.J.M. Westerhof, D.W.F. Brilman, W.P.M. Swaaij, S.R.A. Kersten, Effect of temperature influidised bed fast pyrolysis of biomass: oil quality assessment in test units. Industrial &Engineering Chemistry Research 49 (2010) 1160-1168.

[25] D.C. Elliott, T.R. Hart, G.G. Neuenschwander, L.J. Rotness, A.H. Zacher, Catalytic hydroprocessing of biomass fast pyrolysis bio-oil to produce hydrocarbon products. Environmental Progress & Sustainable Energy 28 (2009) 441-449.

[26] Y. Wang, D. Mourant, X. Hu, S. Zhang, C. Lievens, C.-Z. Li, Formation of coke during the pyrolysis of bio-oil. Fuel 108 (2013) 439-444.

[27] C.Z. Li, F. Wu, H.Y. Cai, R. Kandiyoti, UV fluorescence spectroscopy of coal pyrolysis tars, Energy & Fuels 8 (1994) 1039-1048.

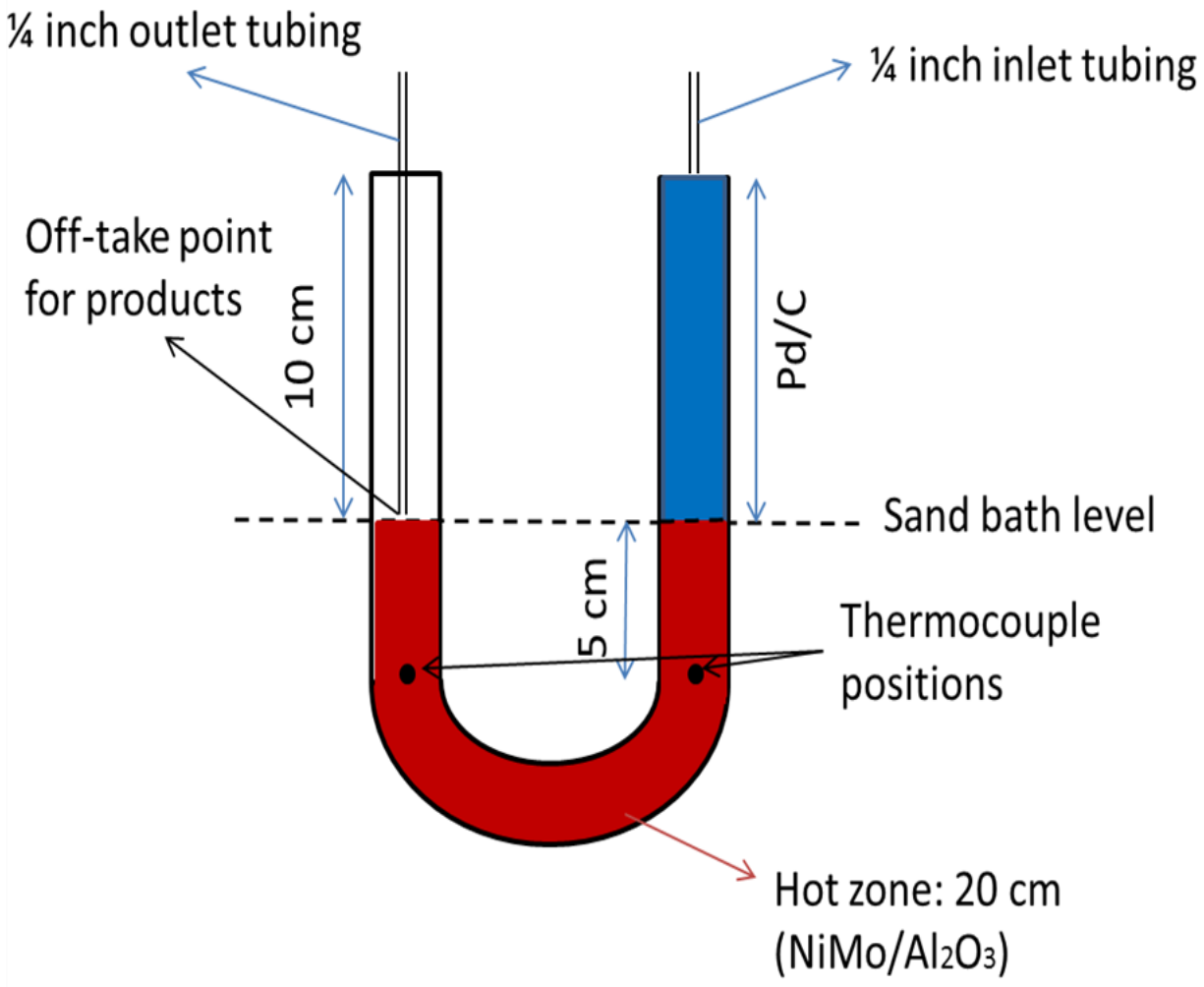

Figure 1 A schematic diagram showing the reactor configuration.

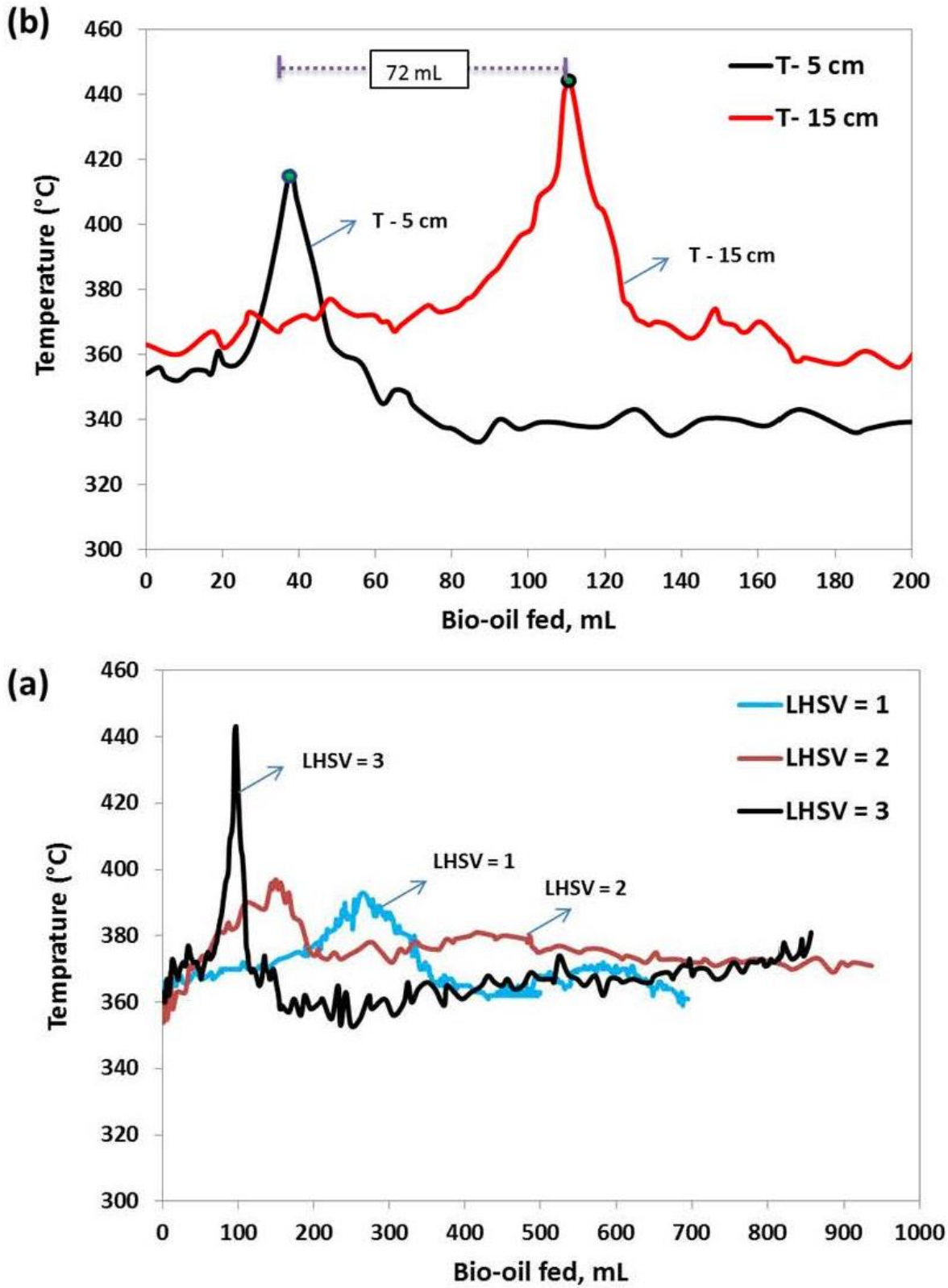

Figure 2 (a) The temperature profiles measuredat the location 15 cm into the $NiMo/Al_2O_3$catalyst bed as a function of LHSV (hr^{-1}). (b) The temperature profiles measured at 5 cm and 15 cm into the $NiMo/Al_2O_3$ catalyst bed for LHSV = 3 hr^{-1}.

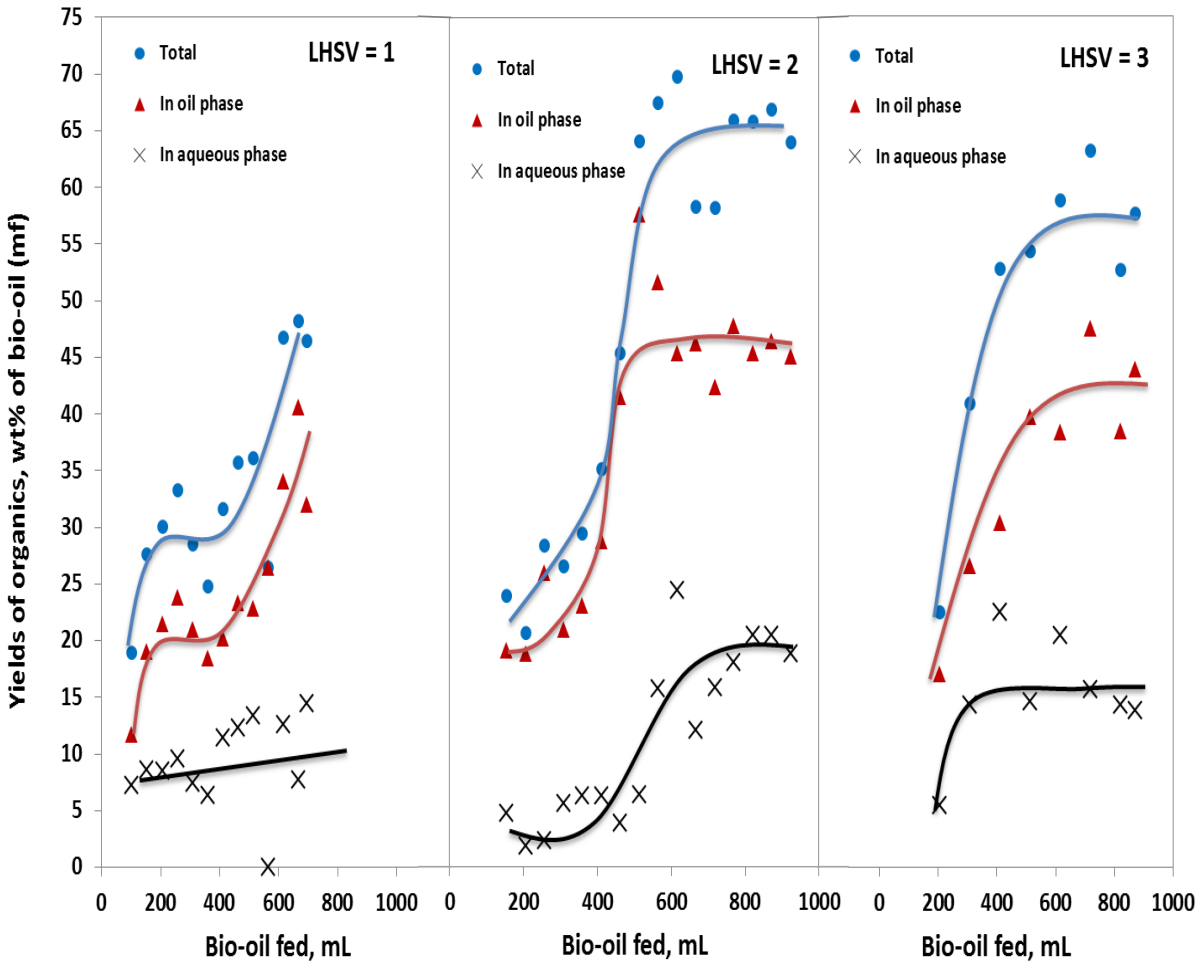

Figure 3 The yields of organics from the hydrotreatment of bio-oil as a function of the volume of bio-oil fed into the reactor and LHSV (hr^{1}).

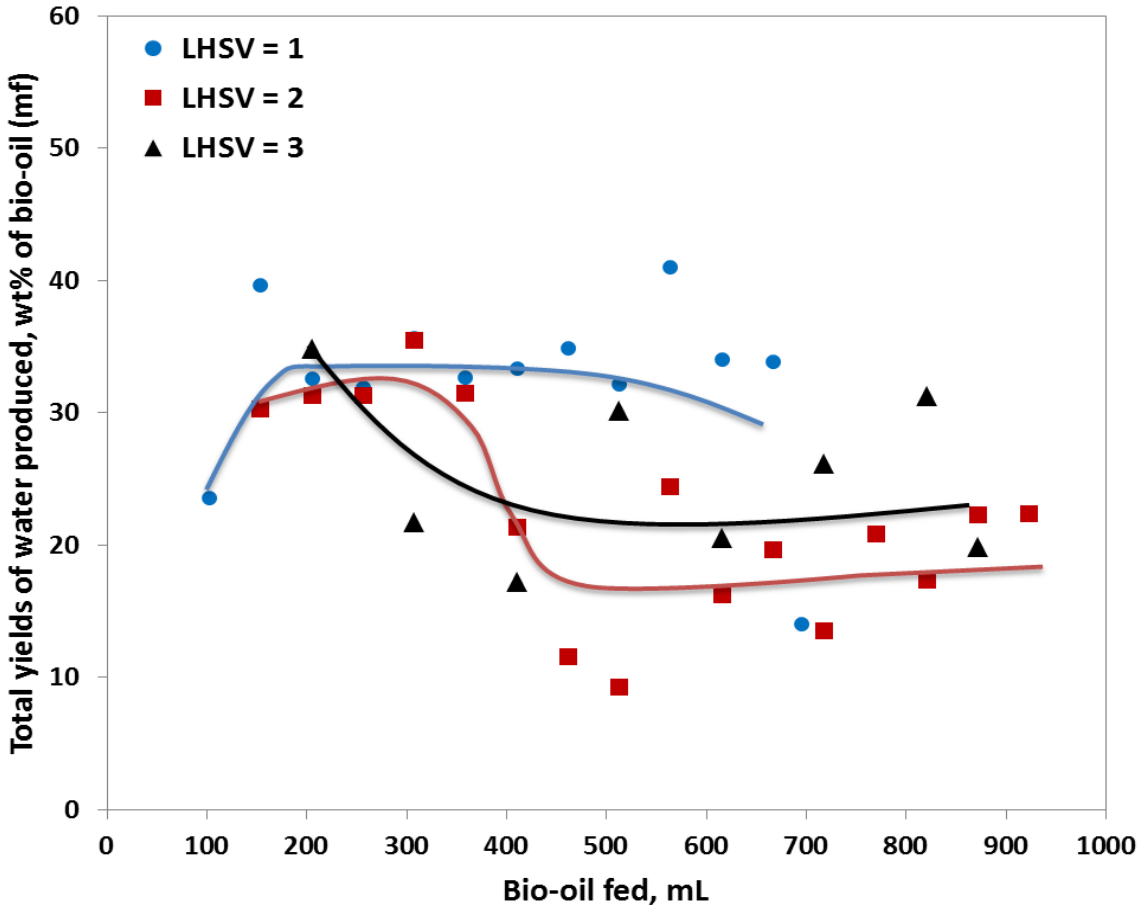

Figure 4 The total water produced as a function of the amount of bio-oil fed into the reactor and LHSV (hr^{1}).

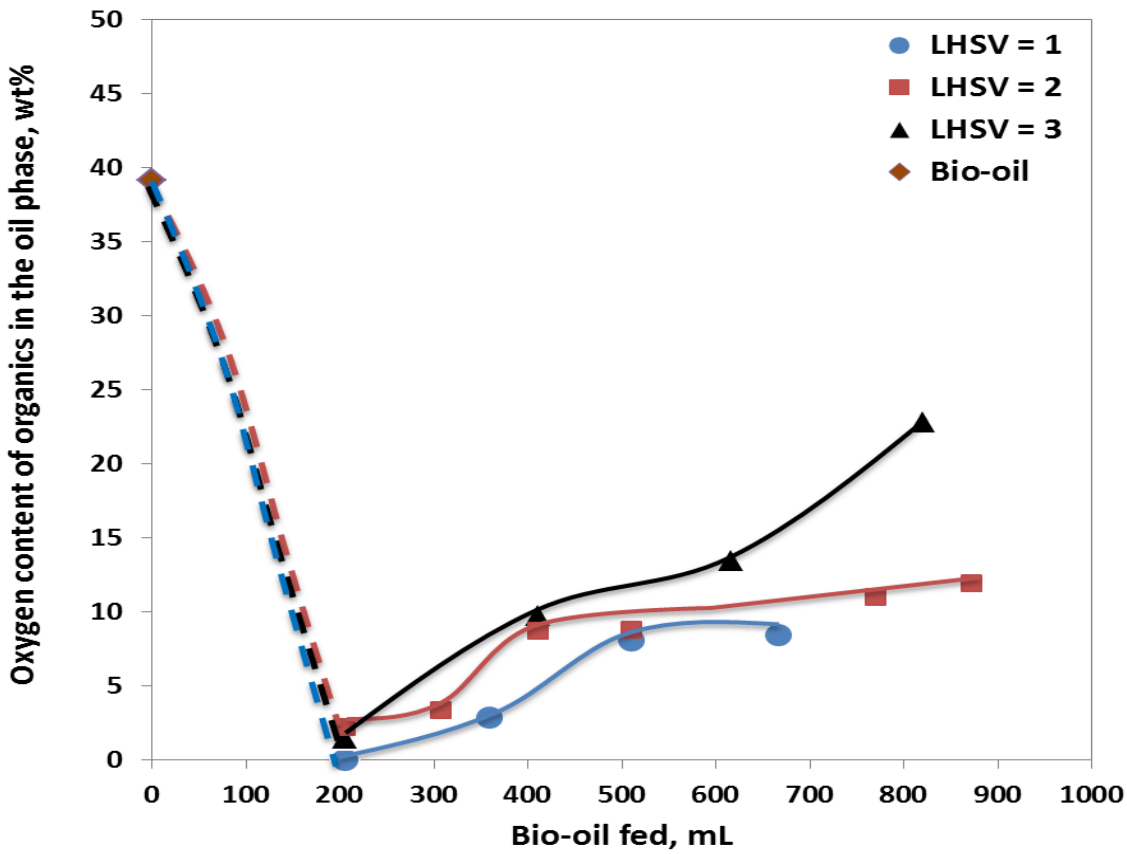

Figure 5 The oxygen content of the organics in the oil phase as a function of the amount of bio-oil fed into the reactor and LHSV (hr^{-1}).

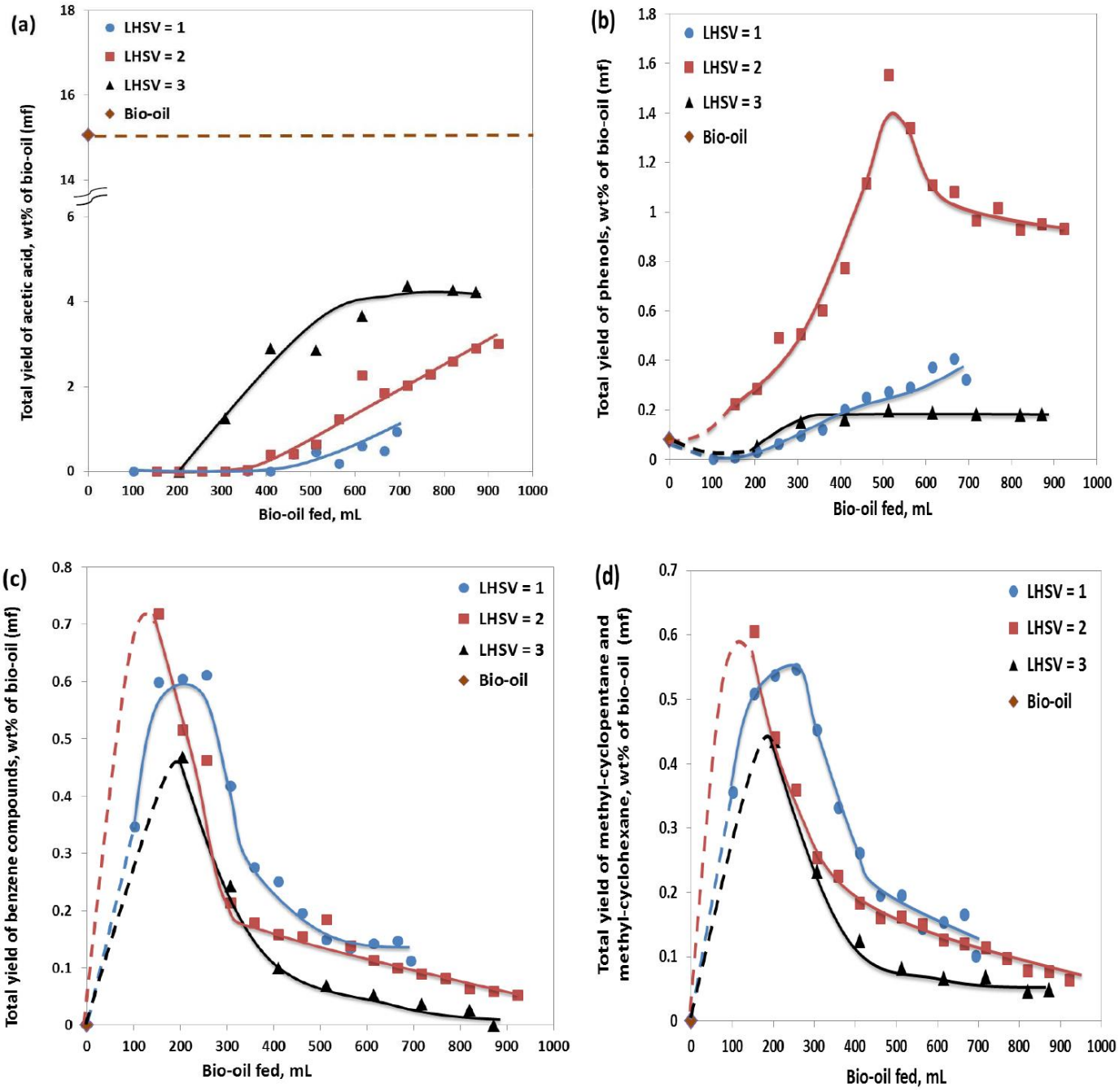

Figure 6 The yields of lighter species from the hydrotreatment of bio-oil as a function of the amount of bio-oil fed into the reactor and LHSV (hr^{-1}).

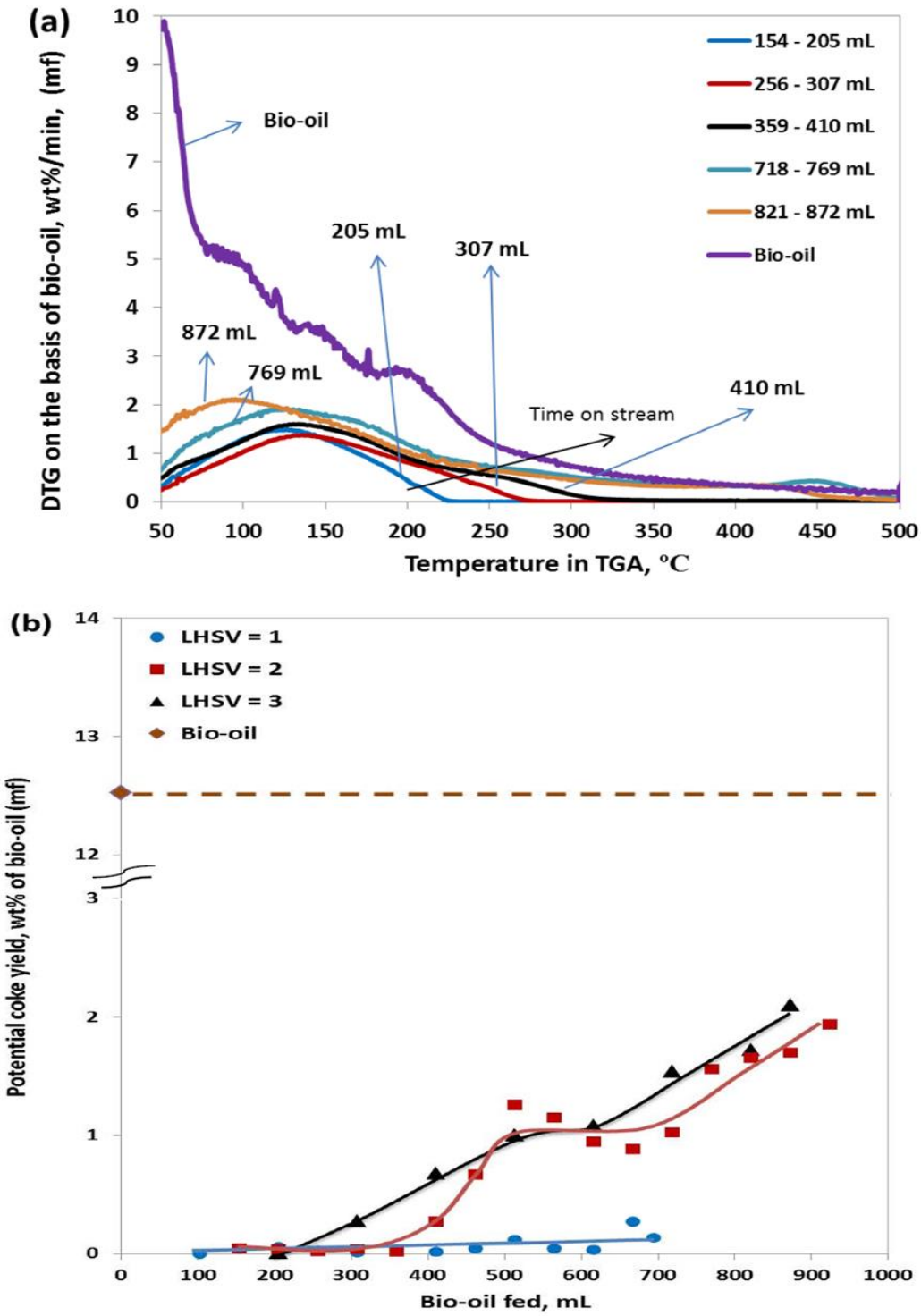

Figure 7 (a), DTG curves of the hydrotreated bio-oils (oil phases) produced at a LHSV of 2 hr^{-1} as a function of the catalyst time-on-stream (reflected by the amount of bio-oil fed into the reactor with intervals labelled in the figure). (b), The potential coke yields of the hydrotreated bio-oils (oil phases) measured by TGA as a function of the catalyst time-on-stream (reflected by the amount of bio-oil fed into the reactor) and LHSV (hr^{-1}).

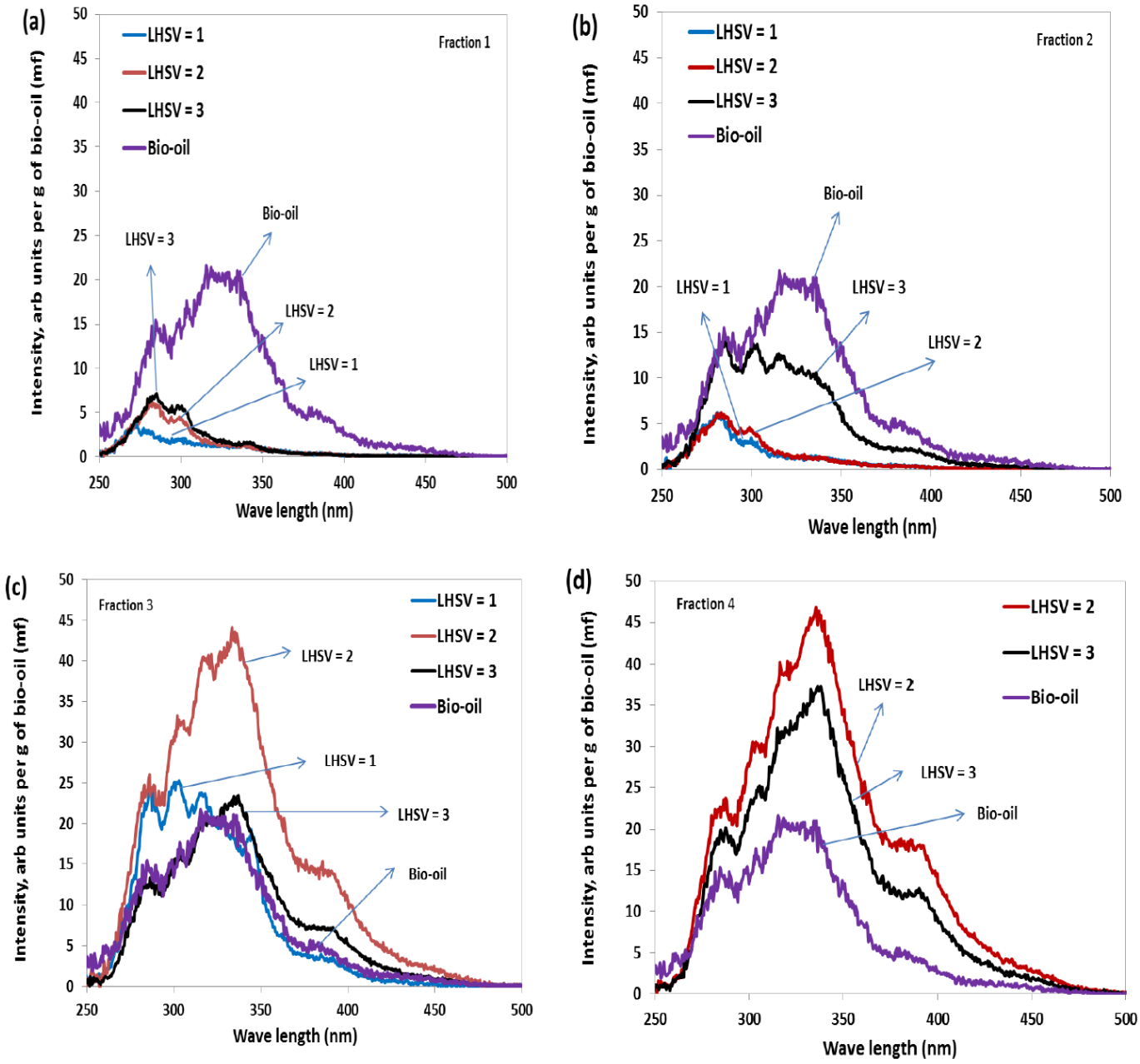

Figure 8 UV fluorescence synchronous spectra as a function of LHSV (hr^{-1}) and catalyst time-on-stream (reflected by the amount of bio-oil fed into the reactor). Note: Fraction 1: 103 – 205 mL bio-oil fed in, Fraction 2: 205 – 307 mL bio-oil fed in, Fraction 3: 513 – 615 mL bio-oil fed in and Fraction 4: 715 – 820 mL bio-oil fed in.